The Effect of Transmission Ratio and the Number of Teeth on Involute Spur Gear Geometrical Characteristics, Load Sharing Ratio, and Contact Stress

Nassear Rahseid Hmoad
Department of Aeronautical Engineering, University of Baghdad, Iraq
naseer.rasheed@coeng.uobaghdad.edu.iq (corresponding author)

Aveen Ahmed Abdulkareem
Department of Mechanical Engineering, University of Baghdad, Iraq
aveen.ahmed@coeng.uobaghdad.edu.iq

Received: 7 April 2025 | Revised: 30 April 2025 | Accepted: 4 May 2025

Licensed under a CC-BY 4.0 license | Copyright (c) by the authors | *DOI: https://doi.org/10.48084/etasr.11358*

ABSTRACT

Among the numerous gear advantages, the speed ratio plays an important role in transmitting mechanical power and control tooth geometry, which is in turn affect the bending and contact tooth strength. The aim of this work is to study the geometry of involute teeth for a different teeth number and speed ratio regarding the second moment of mass numerically, in addition to the investigating the induced contact stress analytically based on the Hertz contact model, and numerically using the Finite Element Method (FEM). The bending stress for the mating teeth has been investigated numerically for their loaded sides. The parameters studied are the pressure angles, speed ratio and gear teeth number, as well as the contact ratio and load sharing. The results show that in general increasing the speed ratio decreases the contact stress for different pressure angles. Higher pressure angles have lower induced bending and contact stresses at a contact ratio lower than 9. However, a larger contact ratio increases the 14.5^o teeth strength, where the shared load reduced by about 33%.

Keywords- spur gears; involumetry; speed ratio; load sharing; contact stress; bending stress

I. INTRODUCTION

Gears are fundamental components in mechanical engineering, extensively utilized in applications, involving power transmission, motion control, and timing mechanisms. Their configurations vary according to the tooth profile and alignment with the axis of rotation, offering flexibility in functions, such as reversing the direction of rotation, adjusting the speed ratios, and redirecting the power transmission paths. A great amount of research has been devoted to improving the gear performance in terms of mechanical strength, wear resistance, vibration suppression, and noise reduction, while also addressing manufacturing and operational cost efficiency [1].

Authors in [2] analyzed the impact of profile modifications on single-tooth load distribution. The impact of periodic contact stresses on tooth failure has been shown to gradually diminish the load-bearing capability of the system [3]. The influence of backlash and manufacturing imperfections on dynamic loads was evaluated using nonlinear multibody simulations, offering guidance on selecting suitable contact parameters, such as the friction coefficient, damping ratio, and stiffness [4].

Authors in [5] performed analytical estimations of transmission errors in spur gears with high contact ratios. The evolution of the contact path on tooth surfaces during meshing cycles has been investigated in [6]. Finite element analysis has been employed to examine the changes in contact pressure between meshing teeth [7], and a new approach for assessing the contact stress during gear engagement has also been proposed [8]. The surface fatigue life in gear pumps has been evaluated using the cumulative damage theory in combination with FEM simulations [9].

The dimensional difference between gear and pinion, typically expressed through the speed ratio, has been extensively studied for its impact on the tooth strength. Building on this foundation, the present work explores the combined influence of the speed ratio and number of teeth on critical geometrical and mechanical parameters, including the contact ratio, tooth profile, load distribution, induced contact and bending stresses, as well as moment of inertia.

The analytical framework employs the Hertzian contact theory to estimate the contact stress based on geometric relations and material properties. Complementary numerical simulations, conducted using FEM, are utilized to validate the analytical results and to evaluate gear geometry parameters, such as volume and moment of inertia, taking into account the element type and count, boundary conditions, and the distribution of transmitted torque.

II. SPUR GEAR SPEED RATIO

Spur gear is considered the oldest gear type and the most widely used due to its ease of design and manufacturing accompanied by high efficiency. The most significant parameters that control its geometry are the pressure angle, module, number of teeth, face width, speed ratio, and fillet radius [10]. The most important relations are:

$$m = D/z \tag{1}$$

$$h_a = m \tag{2}$$

$$h_d = 1.25\, h_a \tag{3}$$

$$R_p = 0.5mz \tag{4}$$

$$c = R_{pp} + R_{pg} \tag{5}$$

$$R_a = R_p + h_a \tag{6}$$

$$R_b = R_p - m \tag{7}$$

$$\rho = R_p \sin\alpha \tag{8}$$

One of the primary objectives of a gear drive is to modify the transmitted torque and angular velocity. To achieve this, the mating gears are designed with different pitch radii, and the ratio of these radii is defined as the speed ratio *(Sr)* [11], expressed as:

$$S_r = z_2/z_1 \tag{9}$$

Increasing the speed ratio significantly affects the gear geometry. Specifically, it alters the tooth profile, making the teeth wider at the root and flatter near the pitch point, while also increasing the overall size of the gear set. These geometric changes are critical for determining the tooth strength and the gear's ability to withstand operational loads. Among these effects, the speed ratio has a particularly strong influence on load sharing between meshing teeth [12]. An increase in the gear size also leads to a higher moment of inertia, which in turn raises the power consumption during transient conditions, a factor that will be analyzed in this study. Additionally, excessive gear noise can negatively impact system performance, while in some applications, may even interfere with human task execution [13]. Since reduced load sharing is associated with lower vibration and noise levels, achieving an effective load distribution is one of the primary goals of this work.

III. LOAD SHARING

The operational behavior of gears is characterized by the continuous engagement of successive teeth during which the transmitted load is distributed among the teeth that are in contact at any given moment. The key parameter governing this load distribution is the contact ratio *(Cr),* which is defined as [14]:

$$Cr = \frac{\sqrt{R_{a2}^2 - R_{b2}^2} + \sqrt{R_{a1}^2 - R_{b1}^2} - (R_{p1} + R_{p2}) \sin\alpha}{\pi m \cos\alpha} \tag{10}$$

In this context, subscripts 1 and 2 denote the pinion and gear, respectively, while α represents the pressure angle. By substituting (2) through (6) into (9), the contact ratio can be formulated as:

$$Cr = \frac{\sqrt{A} + \sqrt{B} - 0.5\, z_1 m\, (1 + s_r) \sin\alpha}{\pi m \cos\alpha} \tag{11}$$

where A, B corresponds/correspond to:

$$\begin{cases} A = m^2(0.025(z_1 s_r)^2(\sin\alpha)^2 + (z_1 s_r) + 1) \\ B = m^2(0.025{z_1}^2(\sin\alpha)^2 + z_1 + 1) \end{cases}$$

It is evident that the contact ratio depends on significant gear design parameters, including the module, number of teeth, pressure angle, and speed ratio. In most practical gear applications, the contact ratio typically ranges between 1 and 2. This implies that, during operation, the number of teeth in contact varies from one to two. The highest load concentration occurs when contact takes place near the pitch point, where only a single tooth carries the entire load [15]. Figures 1 and Figure 2 illustrate the maximum load values for single and double-tooth contact when *Cr<2,* while Figures 3 and 4 correspond to the condition *Cr=2.*

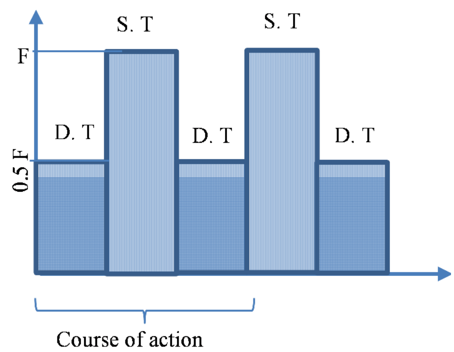

Fig. 1. Tooth maximum load value for single and double tooth contact, Cr<2.

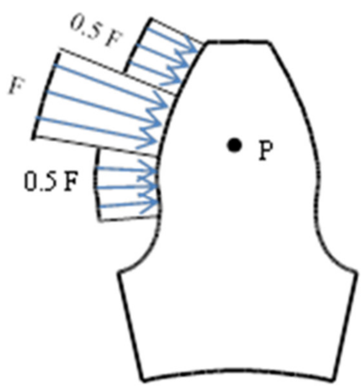

Fig. 2. Transmitted load distribution along the tooth profile, Cr<2.

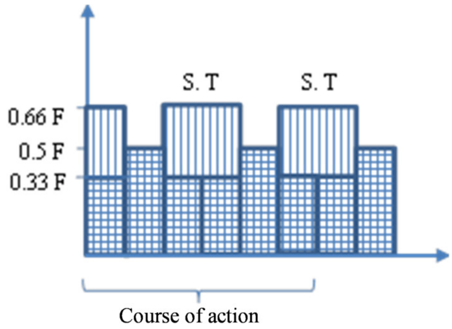

Fig. 3. Tooth maximum load value for single and double tooth contact, Cr=2.

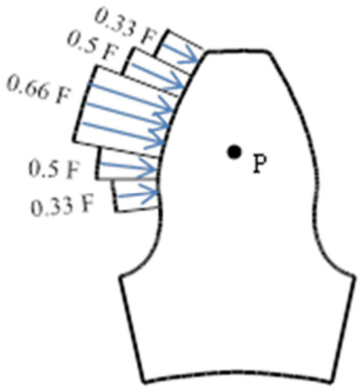

Fig. 4. Transmitted load distribution along tooth profile, Cr=2.

IV. CONTACT STRESS

One of the predominant failure modes in gears is surface degradation, often caused by manufacturing defects, improper installation, or harsh environmental conditions. Among the various factors affecting gear wear, the accurate estimation of contact stress is one of the most critical challenges in predicting and assessing the wear behavior [16]. Wear plays a key role in determining the service life of the moving mechanical components [17].

Due to the repeated occurrence of high localized contact pressure and relative sliding, gear teeth gradually wear down, eventually deviating from their original involute profile. In some cases, wear may partially compensate for minor misalignments in gear meshing [18]. In general, gear tooth contact is evaluated using the Hertzian theory, which models the interaction between two cylindrical bodies with parallel axes. This assumption is most valid near the pitch point, where the contact stress is the highest and the relative sliding between mating teeth is negligible [19]. The induced contact stresses between two aligned cylindrical surfaces are primarily determined by the mechanical properties of the materials and the geometry of the contact surfaces, and are given by [20]:

$$\sigma_c = \sqrt{\frac{F^*}{E^*}} \tag{12}$$

where F^*, E^* correspond to:

$$\begin{cases} F^* = 4\, F_n \left(\frac{1}{R_1} + \frac{1}{R_2}\right) \\ E^* = b\pi \left(\frac{1-\nu_1^2}{E_1} + \frac{1-\nu_2^2}{E_2}\right) \end{cases}$$

V. FINITE ELEMENT MODEL

Given its broad range of capabilities including the analysis of vibration, stress, wear, and even aerodynamics, FEM has become an essential and widely accessible tool in modern engineering simulations. Contact stresses can be effectively simulated using a commercial FEM software, such as COMSOL, ANSYS, and other advanced solvers [21].

In the present study, ANSYS Mechanical APDL is employed to construct 3D models of spur gear teeth under varying design parameters. Each model represents a single pinion tooth meshing with a single gear tooth. The effect of the speed ratio and consequently the contact ratio is incorporated through the application of the corresponding transmitted load on the tooth. The primary outputs of the FEM analysis include the moment of inertia, bending stress, and contact stress. The mechanical properties and microstructure of steel are important in evaluating the structural integrity of the components operating under severe thermal and mechanical conditions [22]. In this analysis, both the gear and the pinion are assumed to be made of the same steel material, with a modulus of elasticity of 200 GPa and a Poisson's ratio of 0.3. The models are discretized using solid brick elements, which are particularly well-suited for simulating rotors, bearings, and gear components [23].

All cases are based on a module of 7mm, face width of 56mm, and a transmitted load of 5.6kN. The contact analysis is performed in 2D using target element type 170 and contact element type 174 for the mating surfaces. The optimal mesh consists of 2400 brick elements and approximately 200 elements, each for the target and contact surfaces. In the simulation setup, the gear is fixed, while the pinion is allowed to rotate about its axis. The results obtained for contact stress will be compared with and validated against theoretical calculations

VI. RESULTS AND DISCUSSION

The analytical results were derived using the fundamental equations for contact ratio and contact stress, while the numerical analysis was conducted using ANSYS Mechanical APDL 15. Graphical representations of the outcomes are used to facilitate interpretation, with emphasis given on identifying both advantageous and detrimental effects across the design scenarios. Improvement percentages are also calculated to quantify the influence of the design parameters. Figure 5 illustrates the effect of the speed ratio on the moment of inertia for different pressure angles, based on finite element analysis. As expected, increasing the speed ratio leads to a higher moment of inertia due to the increase in the pitch radius and tooth size. Specifically, a tenfold increase in the speed ratio results in an approximate 150% increase in inertia across all pressure angles. Among them, the gears with a 14.5° pressure angle exhibit the lowest inertia, which is attributed to their more compact tooth profiles compared to those with higher pressure angles.

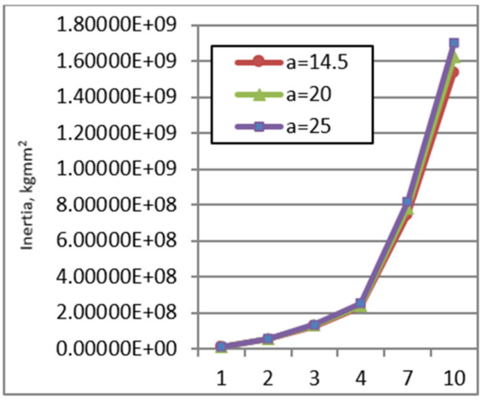

Fig. 5. Effect of speed ratio on gear teeth inertia per unit density and unit width for different ressure angles.

The influence of tooth number and speed ratio on the contact ratio is explored in Figures 6 and 7. Figure 6 displays how the number of teeth affects the contact ratio under unity speed ratio for different pressure angles, while Figure 7 demonstrates the impact of varying speed ratios with a fixed pinion tooth count ($z_1=14$). A contact ratio of 2 can be achieved using 14.5° pressure angle teeth within the studied range, while such a value is unattainable with greater pressure angles due to their shorter line of contact. In Figure 6, for $z_1=z_2=36$, the contact ratio reaches 2, and the corresponding center distance, as determined from (4) and (5), is 252 mm. In contrast, Figure 7 shows that a contact ratio of 2 is also achieved at $z_1=14$ and speed ratio $Sr=9$, yielding a center distance of 490 mm. These findings suggest that achieving a high contact ratio is possible either by increasing the number of teeth or by adjusting the speed ratio. However, opting for more teeth at unity speed ratio results in a 48.5% reduction in gear radius, enabling a more compact design. This size advantage, though, comes with a trade-off, as $Sr=1$ implies no change in angular velocity between the gear and pinion.

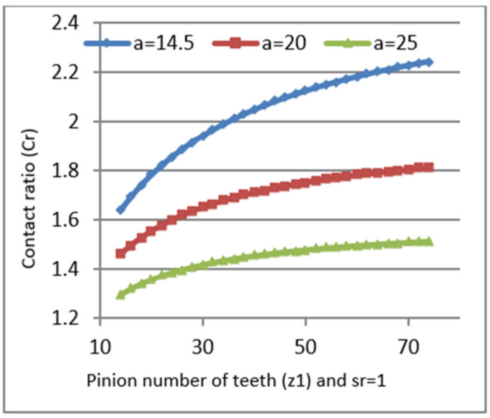

Fig. 6. Effect of teeth number on contact ratio for different pressure angles.

Figures 8 and Figure 9 present the calculated contact stress for different combinations of tooth number and speed ratio, considering various pressure angles. For speed ratios below 9 or at unity speed ratio with fewer than 36 teeth, higher pressure angles (20° and 25°) provide greater strength due to their more robust tooth geometry. These profiles offer increased root thickness and larger radii of curvature, resulting in improved stress distribution. Conversely, at higher speed ratios ($Sr \geq 9$) or when the tooth count reaches or exceeds 36 under unity speed ratio, gears with a 14.5° pressure angle outperform their counterparts. This is attributed to their higher contact ratio of 2, which ensures that two teeth remain in contact throughout the meshing cycle, effectively reducing the load borne by each tooth by approximately 33.3%.

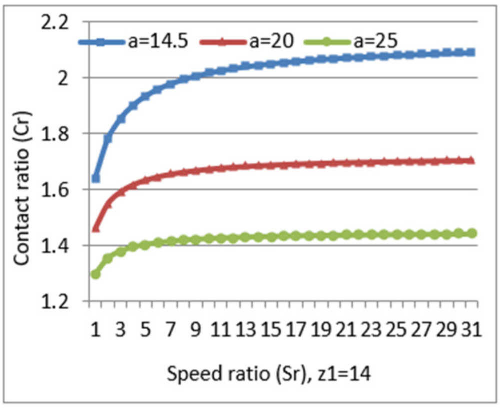

Fig. 7. Effect of speed ratio on contact ratio for different pressure angles.

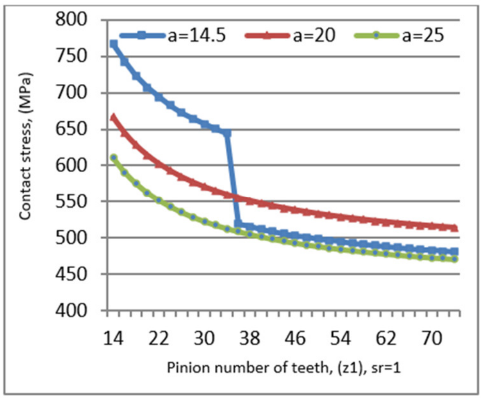

Fig. 8. Effect of speed ratio on contact ratio for different pressure angles.

The numerical analysis confirms the analytical results. For $Sr=1:3$, increasing the pressure angle from 14.5° to 25° reduces the bending stress by approximately 50 % in the pinion and 40% in the gear, and the contact stress by 28 %, due to thicker tooth roots, reduced tangential forces, and larger curvature radii. For $Sr=1:9$, the 14.5° teeth exhibit lower stresses than those with a 20° angle, emphasizing the advantage of high contact ratios, where load sharing reduces the peak stress at the pitch point.

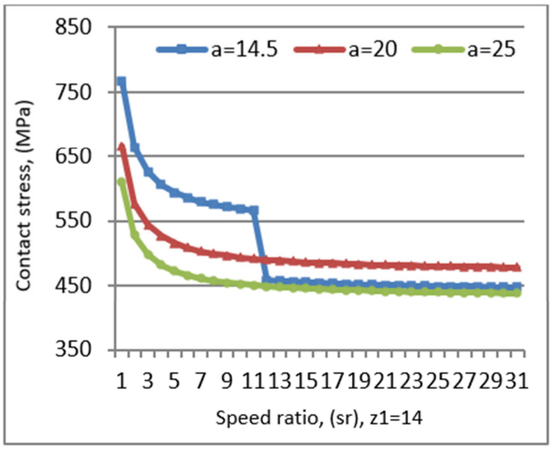

Fig. 9. Effect of teeth number on contact stress for different pressure angles.

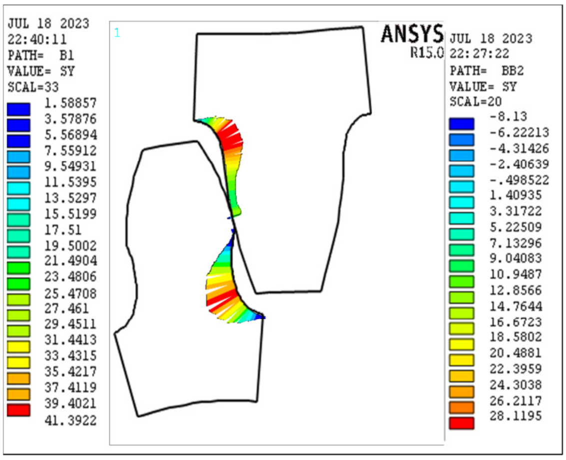

Fig. 10. Bending stress (MPa), α = 14.5°, S_r= 1:3, z_1=14, Cr<2.

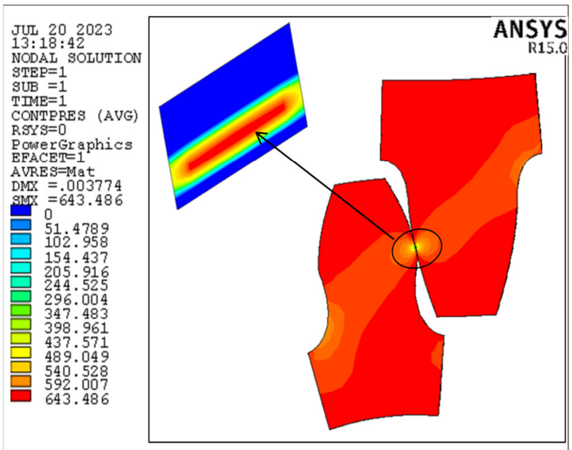

Fig. 11. Contact stress (MPa), α = 14.5°, S_r= 1:3, z_1=14, Cr<2.

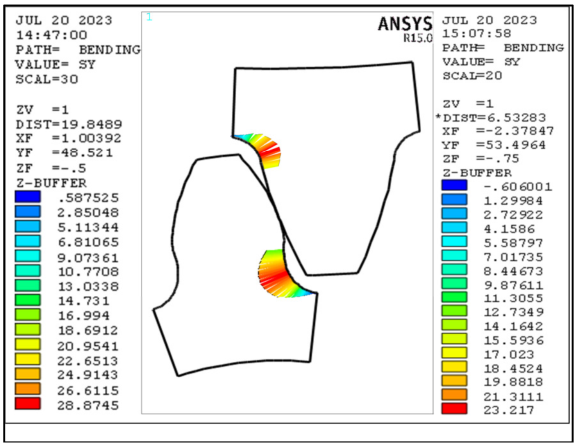

Fig. 12. Bending stress (MPa), α = 20°, S_r= 1:3, z_1=14, Cr<2.

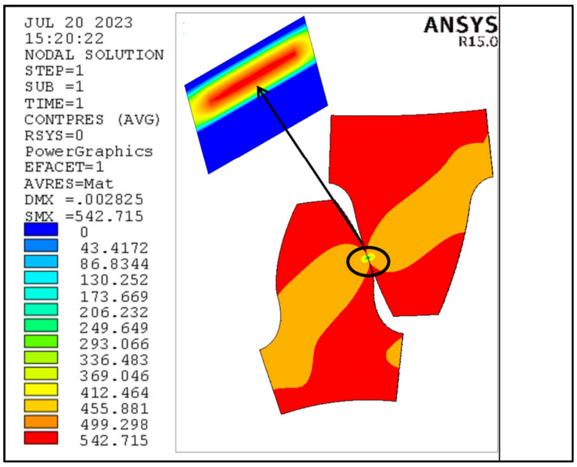

Fig. 13. Contact stress (MPa), α = 20°, S_r= 1:3, z_1=14, Cr<2.

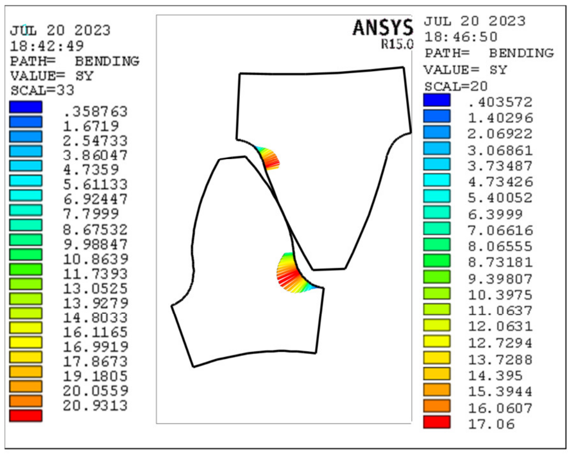

Fig. 14. Bending stress (MPa), α = 25°, S_r= 1:3, z_1=14, Cr<2.

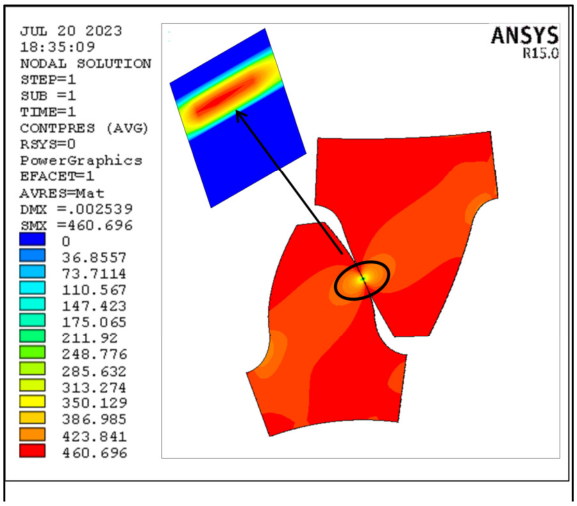

Fig. 15. Contact stress (MPa), α = 25^o, S_r= 1:3, z_1=14, Cr<2.

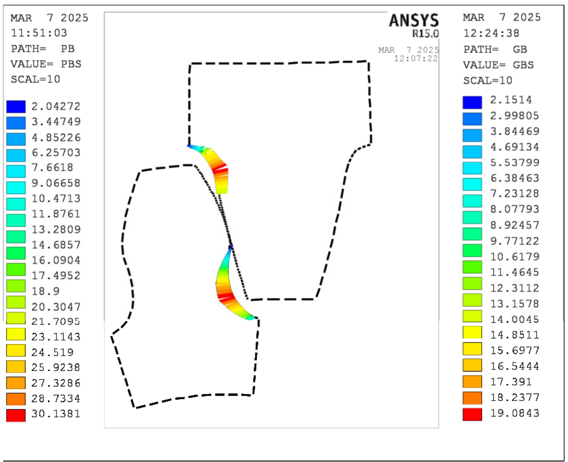

Fig. 16. Bending stress (MPa), α = 14.5^o, S_r= 1:9, z_1=14, Cr=2.

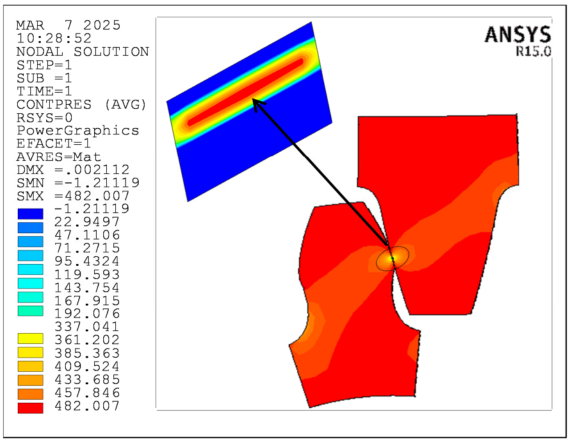

Fig. 17. Contact stress (MPa), α = 14.5^o, S_r= 1:9, z_1=14, Cr=2.

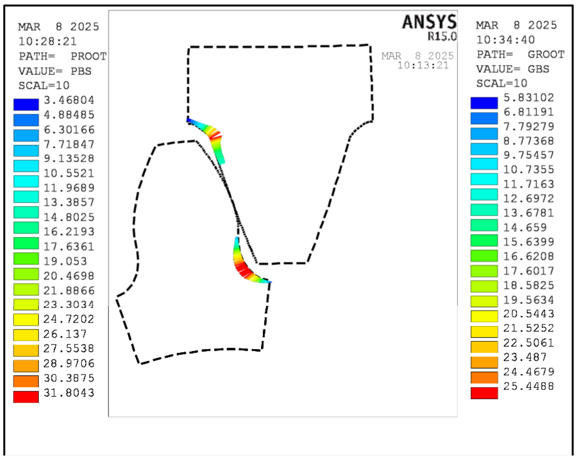

Fig. 18. Bending stress (MPa), α = 20^o, S_r= 1:9, z_1=14, Cr<2.

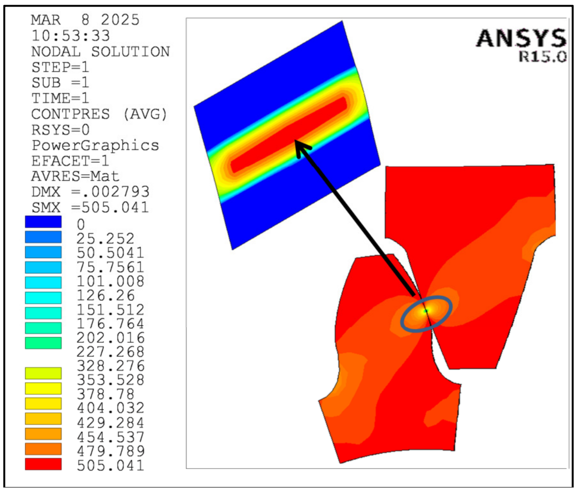

Fig. 19. Contact stress (MPa), α = 20^o, S_r= 1:9, z_1=14, Cr<2.

In general, across all studied cases, the difference in bending stress between mating teeth (pinion and gear) increases as the contact ratio decreases. This trend is more pronounced at lower pressure angles, where fewer teeth are engaged simultaneously, leading to greater load concentration, and thus increased stress disparity between the two components.

VII. CONCUSION

Based on the analytical and numerical results presented in this study, several key conclusions can be drawn regarding the influence of the pressure angle, speed ratio, and contact ratio on the spur gear performance. For speed ratios less than 9, higher pressure angles generally result in increased bending and contact strength due to their inherently more robust tooth geometry. However, at higher speed ratios, specifically in the range *9≤Sr≤31*, lower pressure angles are more favorable, as they lead to reduced contact stress and improved load distribution through higher contact ratios. Within the examined design ranges, it was observed that a higher contact ratio can be achieved using a greater number of teeth at a unity speed ratio rather than increasing the speed ratio itself. This approach allows for a significant reduction in the gear size without sacrificing contact performance, thereby contributing to lower power consumption. Furthermore, the results indicate that as the contact ratio increases, so does the difference in bending stresses. This disparity becomes more pronounced at lower pressure angles, where fewer teeth are in contact simultaneously.

These findings provide valuable insights for optimizing spur gear design under varying operating conditions, balancing strength, compactness, and efficiency.

NOMENCLATURE

b	Gear face width (mm)
c	Center distance (mm)
Cr	Contact ratio
D	Pitch diameter (mm)
E	Modulus of elasticity (GPa)
F	Tangential force (N)
Fn	Normal force (N)
h	Tooth height (mm)
h_a	Addendum (mm)
h_d	Dedendum (mm)
m	Module (mm)
R_1	Inion pitch radii (mm)
R_2	Gear pitch radii (mm)
Ra	Addendum radii (mm)
Rb	Base radii (mm)
Sr	Speed ratio
z_1	Number of teeth
z_2	Number of teeth
α	Pressure angle (deg.)
v_1	Pinion Poisson's ratio
v_2	Gear Poisson's ratio
σ_c	Contact stress (MPa)

REFERENCES

[1] A. W. Hussein and M. Q. Abdullah, "A Novel Fillet Form for Non-Generation Cutting Gear Teeth," *Results in Engineering*, vol. 16, Dec. 2022, Art. no. 100523, https://doi.org/10.1016/j.rineng.2022.100523.

[2] H. Winter and T. Placzek, "Load distribution and topological flank modification of helical and double helical gears," *European Journal of Mechanical Engineering*, vol. 36, no. 3, pp. 171-176, 1991.

[3] P. J. L. Fernandes and C. McDuling, "Surface contact fatigue failures in gears," *Engineering Failure Analysis*, vol. 4, no. 2, pp. 99–107, Jun. 1997, https://doi.org/10.1016/S1350-6307(97)00006-X.

[4] A. Sommer, J. Meagher, and X. Wu, "An Advanced Numerical Model of Gear Tooth Loading from Backlash and Profile Errors," in *Rotating Machinery, Structural Health Monitoring, Shock and Vibration, Volume 5*, New York, NY, USA, 2011, pp. 191–201, https://doi.org/10.1007/978-1-4419-9428-8_15.

[5] R. G. Munro, L. Morrish, and D. Palmer, "Gear transmission error outside the normal path of contact due to corner and top contact," *Proceedings of the Institution of Mechanical Engineers, Part C: Journal of Mechanical Engineering Science*, vol. 213, no. 4, pp. 389–400, Apr. 1999, https://doi.org/10.1243/0954406991522347.

[6] G. I. Sheveleva, A. E. Volkov, and V. I. Medvedev, "Algorithms for analysis of meshing and contact of spiral bevel gears," *Mechanism and Machine Theory*, vol. 42, no. 2, pp. 198–215, Feb. 2007, https://doi.org/10.1016/j.mechmachtheory.2006.02.009.

[7] S.-C. Hwang, J.-H. Lee, D.-H. Lee, S.-H. Han, and K.-H. Lee, "Contact stress analysis for a pair of mating gears," *Mathematical and Computer Modelling*, vol. 57, no. 1, pp. 40–49, Jan. 2013, https://doi.org/10.1016/j.mcm.2011.06.055.

[8] T. Jabbour and G. Asmar, "Tooth stress calculation of metal spur and helical gears," *Mechanism and Machine Theory*, vol. 92, pp. 375–390, Oct. 2015, https://doi.org/10.1016/j.mechmachtheory.2015.06.003.

[9] H. Shen, Z. Li, L. Qi, and L. Qiao, "A method for gear fatigue life prediction considering the internal flow field of the gear pump," *Mechanical Systems and Signal Processing*, vol. 99, pp. 921–929, Jan. 2018, https://doi.org/10.1016/j.ymssp.2016.09.022..

[10] C. S. Sharma and K. Purohit, *Theory of Mechanisms and Machines*, 6th ed. New Delhi, India: PHI Learning Private Limited, 2006.

[11] L. Liu, L. Zhu, and X. Gou, "Modeling and analysis of load distribution ratio and meshing stiffness for orthogonal spur-face gear drive under point contact," *Mechanism and Machine Theory*, vol. 182, Apr. 2023, Art. no. 105239, https://doi.org/10.1016/j.mechmachtheory.2023.105239.

[12] J. I. Pedrero, M. B. Sánchez, and M. Pleguezuelos, "Analytical model of meshing stiffness, load sharing, and transmission error for internal spur gears with profile modification," *Mechanism and Machine Theory*, vol. 197, Jul. 2024, Art. no. 105650, https://doi.org/10.1016/j.mechmachtheory.2024.105650.

[13] A. Kaleel, A. Al-hamadani, and K. Kadhim, "Noise effects in skill discretion and modeling," *Journal of Mechanical Engineering Research and Developments*, vol. 43, no. 7, pp. 87–99, Oct. 2020.

[14] G. M. Maitra, *Handbook of Gear Design*, 1st ed. New York, NY, USA: Tata McGraw-Hill, 1994.

[15] S. P. Radzevich, *Theory of Gearing: Kinematics, Geometry, and Synthesis*, 3rd ed. Boca Raton, FL, USA: CRC Press, 2022.

[16] A. R. Breeds, S. N. Kukureka, K. Mao, D. Walton, and C. J. Hooke, "Wear behaviour of acetal gear pairs," *Wear*, vol. 166, no. 1, pp. 85–91, Jun. 1993, https://doi.org/10.1016/0043-1648(93)90282-Q.

[17] -O. Bildik and M. Yaşar, "Manufacturing of Wear Resistant Iron-Steel: A Theoretical and Experimental Research on Wear Behavior," *Engineering, Technology & Applied Science Research*, vol. 11, no. 3, pp. 7251–7256, Jun. 2021, https://doi.org/10.48084/etasr.4092.

[18] T. M. Hammza, "Influence of Blending Nanoparticles with Lubricating Oils on the Performance of Rotor Bearings Systems," *International Review of Mechanical Engineering (IREME)*, vol. 15, no. 10, pp. 545–553, Oct. 2021, https://doi.org/10.15866/ireme.v15i10.21528.

[19] D. G. Zisopol, I. Nae, A. I. Portoaca, and I. Ramadan, "A Theoretical and Experimental Research on the Influence of FDM Parameters on Tensile Strength and Hardness of Parts Made of Polylactic Acid," *Engineering, Technology & Applied Science Research*, vol. 11, no. 4, pp. 7458–7463, Aug. 2021, https://doi.org/10.48084/etasr.4311.

[20] Nassear R. Hmoad, Aveen A. Abdulkareem, Mohammad Q. Abdullah, "Dynamic Load Factor for Single Element Camshaft under Harmonic Excitation," *Journal of Mechanical Engineering Research and Development*, vol. 43, no. 3, pp. 224-234, 2020.

[21] A. Q. Mohammed, I. Y. Hussain, A. H. Ali, and O. I. Abdullah, " Experimental and Numerical Analysis for Thermal Problem of Frictional Brake System," *Computational Thermal Sciences: An International Journal*, vol. 15, no. 4, 2023, https://doi.org/10.1615/ComputThermalScien.v15.i4.50.

[22] A. M. Saadoon, M. A. Gharawi, and A. Al-Mosawe, "Effect of Elevated Temperature on Microstructure and Mechanical Properties of Hot-Rolled Steel," *Engineering, Technology & Applied Science Research*, vol. 14, no. 6, pp. 18756–18766, Dec. 2024, https://doi.org/10.48084/etasr.9108.

[23] T. M. Hammza, N. R. Hmoad, and A. A. Abdulkareem, "The effect of biolubricants oil on the dynamic performance of rotor bearing system," *AIP Conference Proceedings*, vol. 2415, no. 1, Art. no. 040003, Dec. 2022, https://doi.org/10.1063/5.0092281.